Paper

Visual Tracking Method of a Quick and Anomalously Moving Badminton Shuttlecock

Hidehiko Shishido†, Yoshinari Kameda†, Yuichi Ohta (member)†, Itaru Kitahara†

Abstract: This paper introduces a method that uses multiple-view videos to estimate the 3D position of a badminton shuttle that moves quickly and anomalously. When an object moves quickly, it is observed with a motion blur effect. By utilizing the information provided by the shape of the motion blur region, we propose a visual tracking method for objects that have an erratic and drastically changing moving speed. When the speed increases tremendously, we propose another method, which applies the shape-from-silhouette technique, to estimate the 3D position of a moving shuttlecock using unsynchronized multiple-view videos. We confirmed the effectiveness of our proposed technique using video sequences and a CG simulation image set.

Key words: visual tracking, motion blur, Kalman filter, statistical estimation, anomalously moving badminton shuttlecock

1. Introduction

To promote training efficiency and the realization of tactical analysis, in recent years, there has been a move to introduce information processing/analytical technology into sports competition. The visual tracking of moving objects is one of the most important issues for computer vision research. Recent applications have been developed to illuminate tactics and improve their construction levels for sporting events[1) – 3)]. However, to achieve practical applications, various challenges must be mitigated, including the detection of such multiple objects as players and balls that move quickly and anomalously by images captured in large-scale spaces. In this paper, using multiple images, we focus on detecting and stably tracking objects that move quickly and anomalously.

As a tracking target, we focus on a badminton shuttlecock (hereafter called "shuttle"), since it conspicuously presents the above problems. A shuttle is composed of feathers that are adhesively attached to a hemispheric cork. Since it is lighter than the balls used for other sports, attaching a transmitter or a marker for position sensing is too difficult. Tracking a shuttle presents an additional problem. Due to its structure, during a badminton rally, its moving velocity is inconsistent and is drastically altered by air resistance[4)]. When an object moves quickly, its image is observed with a motion blur, as shown in Fig. 2 (b) and (c). Utilizing information provided by the motion blurs, we successfully developed a visual tracking method for an object that erratically and drastically changes its moving speed (Fig. 1)[5)]. However, when the shuttle has just been returned, its speed becomes maximum and it moves anomalously (Fig. 2 (a)). As a result, since accurate ellipsoidal regression, which is needed for estimating the motion blur shape, is impossible, it is difficult to accurately estimate its position and speed by our conventional method. In this paper, we focus on observing a target object (when it moves very fast), as one curved-line by motion blur; we then propose a method that estimates the 3D trajectory by applying the shape-from-silhouette technique with multi-viewpoint images. Because of its eccentricity, the shuttle has a characteristic that its position and posture change anomalously during rotational movement. In this study, anomalous movement refers to a condition accompanied by abrupt movement by the force exerted from the outside of the target object. Therefore, in this paper, a badminton shuttle is an object moving quickly and anomalously.

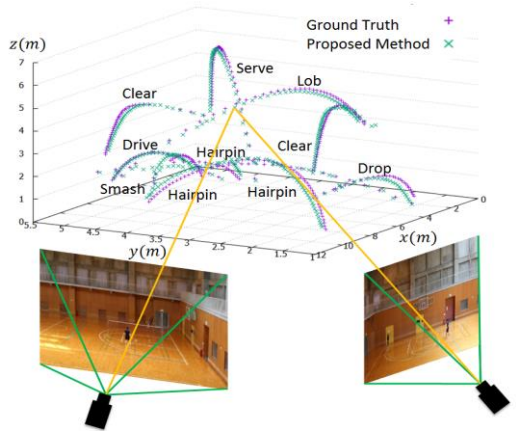

Fig. 1 3D Position estimation results for badminton shuttle utilizing motion blur.

Received ; Revised ; Accepted
†University of Tsukuba
(1–1–1 Tennodai Tsukuba, Ibaraki, Japan)

2. Related Works

Using a super-high-speed camera is a promising approach for tracking a small darting object, such as a microbe or a ball [6) 7)]. However, it is unreasonable to install such a camera for actual badminton games in ordinary gymnasiums. Visual object tracking methods using standard color cameras are also being developed for sporting events[1)–3)]. In the captured images, the ball's observation size is small, it moves quickly, and has just a couple characteristics, such as color and shape. These methods solve the problem by assuming that the ball's motion follows a simple dynamic model and by observing spherical objects, such as a ball, as a circular form in the captured images. Even when the target object is not observed due to occlusion or circumstances such as aggravation of the observation conditions, as decreased resolution, a Kalman filter can compensate for the lost information to estimate the position[8) 9)].

In this paper, we refer to the state (speed) of the shuttle to solve the shuttle-tracking problem with both switching Kalman and particle filters (Section 3). Because the position's observation precision is high when the speed is slow, we input the distance between the observed positions in the former and present frames (observation speed) to the Kalman filter position (observation position). When the speed is fast, we input the observed velocity (observation speed) and the estimated position (observation position) to the Kalman filter (Fig. 3).

However, the shuttle does not follow a simple dynamic model shortly after being struck. In Section 4, we solve this problem by applying a 3D reconstruction method, called shape-from-silhouette[10)], which reconstructs the 3D shape of target objects by combining silhouette images generated from multiple-view images. When the shuttle moves very quickly and anomalously, we estimate its 3D position as a 3D trajectory, rather than an individual position, and we observe it as a single curved-line by the motion blur in the captured images. We call the curved-lines "observation lines" and we extract them from every multiple-view image. We generate a 3D trajectory by combining the extracted observation lines using the shape-from-silhouette technique.

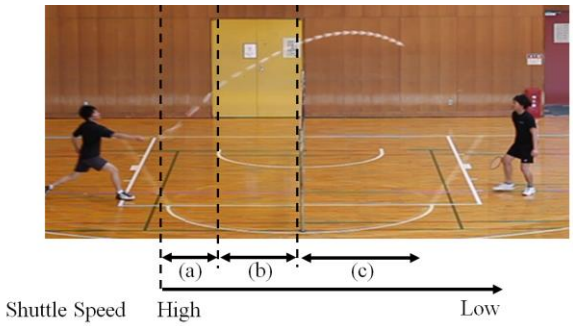

Fig. 2 Examples of appearance of a badminton shuttle with motion blur.

3. Visual Object Tracking Method Utilizing Motion Blur

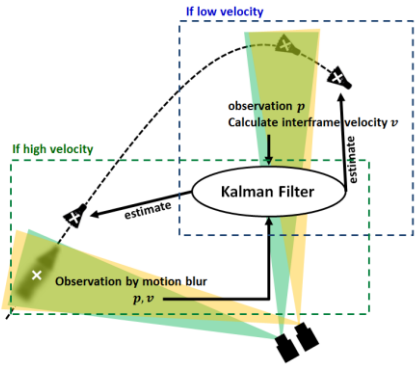

Fig. 3 Visual tracking method of object that variously and drastically changes its moving velocity by motion blur.

3.1 Detection of a Moving Object Region

At the beginning of the object tracking and/or after losing sight of the shuttle, we detect it using the following processes. First, the moving object candidate regions are extracted by background subtraction processing, where the player regions are excluded by referring to the player-region size. We mask out such regions as the court-line and the net where accurate segmentation processing is difficult due to the high brightness level. We execute these processes in frames captured from two viewpoints and calculate the shuttle's 3D position by stereo vision. The shuttle's 3D position is the observed position of the Kalman filter.

3.2 Construction of a Kalman Filter

We use the 3D position, the velocity, and the acceleration for the state of the shuttle in frame k:

$$X_k = \{x_k, \dot{x}_k, \ddot{x}_k, y_k, \dot{y}_k, \ddot{y}_k, z_k, \dot{z}_k, \ddot{z}_k\} \quad (1)$$

The state model of the Kalman filter is denoted by Eq. (2):

$$X_k = AX_{k-1} + Bu_k + \omega_k \quad (2)$$

Here, A is a state transition matrix and the shuttle's

movement forms a parabola with the air resistance:

$$A = \begin{bmatrix} 1 & \delta_t & 0 & 0 & 0 & 0 & 0 & 0 & 0 \\ 0 & 1 & \delta_t & 0 & 0 & 0 & 0 & 0 & 0 \\ 0 & -\frac{c}{m}\delta_t & 0 & 0 & 0 & 0 & 0 & 0 & 0 \\ 0 & 0 & 0 & 1 & \delta_t & 0 & 0 & 0 & 0 \\ 0 & 0 & 0 & 0 & 1 & \delta_t & 0 & 0 & 0 \\ 0 & 0 & 0 & 0 & -\frac{c}{m}\delta_t & 0 & 0 & 0 & 0 \\ 0 & 0 & 0 & 0 & 0 & 0 & 1 & \delta_t & 0 \\ 0 & 0 & 0 & 0 & 0 & 0 & 0 & 1 & \delta_t \\ 0 & 0 & 0 & 0 & 0 & 0 & 0 & -\frac{c}{m}\delta_t & 0 \end{bmatrix} \quad (3)$$

$$B = \begin{bmatrix} 0 & \cdots & 0 & 0 \\ \vdots & \ddots & \vdots & \vdots \\ 0 & \cdots & 0 & 0 \\ 0 & \cdots & 0 & -g \end{bmatrix} \quad (4)$$

δ_t is the time lag between two successive frames. Bu_k is the control input of a state transition. u_k is a vector representing the input to the system. ω_k is process noise by using Gaussian distribution. m is the mass and c expresses the amount of air resistance. Since the acceleration due to gravity g applied in the z direction is not included in the state transition matrix of $\boldsymbol{A}$, matrix $\boldsymbol{B}$ is defined by including this consideration. In comparison, in frame k, when the estimated 3D position of the shuttle becomes p_k, an observation model can be expressed by Eqs. (5) and (6):

$$p_k = \hat{H}_k X_k + \varepsilon_k \quad (5)$$

$$\hat{H}_k = \begin{bmatrix} 1 & 0 & 0 & 0 & 0 & 0 & 0 & 0 & 0 \\ 0 & 1 & 0 & 0 & 0 & 0 & 0 & 0 & 0 \\ 0 & 0 & 0 & 0 & 0 & 0 & 0 & 0 & 0 \\ 0 & 0 & 0 & 1 & 0 & 0 & 0 & 0 & 0 \\ 0 & 0 & 0 & 0 & 1 & 0 & 0 & 0 & 0 \\ 0 & 0 & 0 & 0 & 0 & 0 & 0 & 0 & 0 \\ 0 & 0 & 0 & 0 & 0 & 0 & 1 & 0 & 0 \\ 0 & 0 & 0 & 0 & 0 & 0 & 0 & 1 & 0 \\ 0 & 0 & 0 & 0 & 0 & 0 & 0 & 0 & 0 \end{bmatrix} \quad (6)$$

$$p_k = \begin{cases} x_k, y_k, z_k(BD), \dot{x}_k, \dot{y}_k, \dot{z}_k(IV), \ddot{x}_k, \ddot{y}_k, \ddot{z}_k & if\ Low\ Speed \\ x_k, y_k, z_k(PCG), \dot{x}_k, \dot{y}_k, \dot{z}_k(BV), \ddot{x}_k, \ddot{y}_k, \ddot{z}_k & if\ High\ Speed \end{cases}$$

$BD: background\ difference$

(The moving object candidate regions are extracted by background subtraction processing in frames captured from two viewpoints. The shuttle's 3D position is calculated by stereo vision.)

$IV: interframe\ velocity$

$PCG: particle\ center\ of\ gravity$

$BV: blur\ velocity$

An observation model defines the position and the velocity. ε_k is the random noise that occurs at the time of the observation. The observation noise is a variance matrix computed from the observation error of the observation trajectory acquired manually and a trajectory without observation noise. Based on the velocity gained by the process explained below, observation model $\hat{H}_k$ (based on the object's velocity) is obtained by choosing the observation information given to a Kalman filter.

3.3 Likelihood Calculation Using Color Information

Next, we used color information to calculate the tracked object's likelihood. In this study, the likelihood of the tracked object (shuttle) is defined as the plausible color of the shuttle observed from the captured image. (validity of shuttle). Fig. 4 shows the distribution of the illuminance values in the observed badminton's shuttle regions. The shuttle's illuminance level is affected by the movement blur and the color of the shuttle appears to be mixed with the color of the background.

Since the influence of the movement blur has a linear relation with the velocity, we classify the distribution into three classes (fast, medium, and slow) and determine a likelihood model that corresponds to each velocity. We employ a k-means algorithm as a clustering method. As shown in Fig. 4 (left), the illuminance value of the shuttle observed in the brown background region (gymnasium floor) and the gray background region (gymnasium wall) are well segmented into two clusters. Fig. 4 (right) also shows the clustered results of the observed shuttle illuminance. Since it is significantly influenced by the motion blur, when the shuttle's speed is fast, its color appears mixed with the background color. In the figure's RGB space, it is represented as pink. Similarly, when the shuttle is slow, since there is little influence by the motion blur, it is observed as its original color. In the figure, it is represented by orange. Finally, the middle velocity case is represented by cyan. We classify the distribution into two background regions and three velocity classes.

I. Gymnasium floor, fast velocity
II. Gymnasium floor, medium velocity
III. Gymnasium floor, slow velocity
IV. Gymnasium wall, fast velocity
V. Gymnasium wall, medium velocity
VI. Gymnasium wall, slow velocity

We assume that the distance from the center of gravity of each color class and the shuttle's actual color is a likelihood function and selectively use six kinds of likelihood functions, based on the predictive position and the shuttle's velocity. The output formula of the likelihood function $L(d)$ is presented in Eqs. (7) and (8):

$$L(d_a) = \frac{1}{\sqrt{2\pi}\sigma} exp\left(-\frac{(d_a)^2}{2\sigma^2}\right) \quad (7)$$

$$L(d_b) = \frac{1}{\sqrt{2\pi}\sigma} exp\left(-\frac{(d_b)^2}{2\sigma^2}\right) \quad (8)$$

The likelihood function $L(d)$ is a function of the Euclid distance d from the center of gravity of each color class. We assume that a normal distribution function becomes variance σ^2, which is set based on the sample frame group. $L(d_a)$ is the illuminance values class of the gymnasium floor background region. $L(d_b)$ is the illuminance values class of the gymnasium wall background region. The likelihood function chooses $L(d_a)$ if the shuttle's predictive position is in the brown background region. The gray background region

likelihood function of the court is considered $L(d_b)$.

As shown in Fig. 2, when the shuttle speed is high, under the influence of motion blur, the observed shuttle color is mixed with the background color. In comparison, when the moving speed decreases, it is observed as a white point. Then, it is observed as a color close to the original white color of the shuttle. The luminance distribution was applied in two classes through this preliminary investigation. This presents a challenge since the estimation accuracy of the medium speed shuttle decreases. Stable estimation is realized by dividing it into three classes.

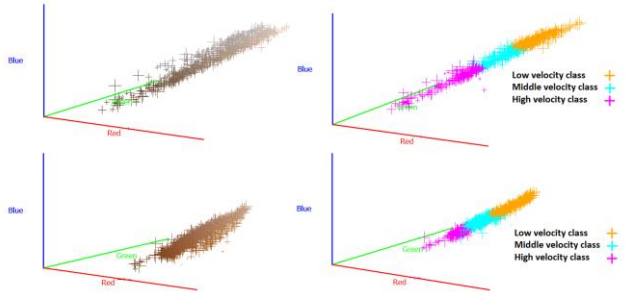

Fig. 4 (Left) Distribution of illuminance values of observed badminton shuttle regions, (Right) clustering of illuminance values of observed shuttle.

3.4 Acquisition of Object's 3D Position and Velocity Using Particles

Our method can statistically estimate an object's 3D position and its velocity information using particles (Fig. 5), which are scattered around a 3D position predicted by a Kalman filter. The initial variance is a range (spherical) of process noise ω_k. The spherical variance range is transformed into an ellipsoid form (Fig. 5 (a)) using a velocity vector predicted by the Kalman filter. We can place a particle in a range where the motion blur is affected with a predictive velocity vector.

Then the method repositions the particle as weighted by the likelihood function's output (Fig. 5 (b)). At this point, the particles in the 3D space express the shape of the motion-blurred shuttle (Fig. 5 (c)). The 3D position of the shuttle is the center of gravity of all of the particles. We can acquire velocity vectors by analyzing the relocation particle's distribution (Fig. 5 (d)) in Eq. (9). The movement velocity v of the shuttle in the 3D position q is calculated by dividing the length of the major axis l and the shutter-speed (opening time) t. Here, the length l of the major axis of an ellipsoid formed by the particles is the distance moved by the shuttle during the shutter opening time t of the capturing camera:

$$v = l \ / \ t \tag{9}$$

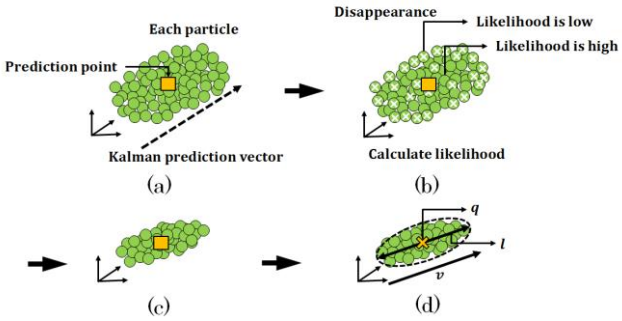

Fig. 5 (a) Transforming a spherical distribution into ellipsoid form, (b) likelihood calculation, (c) particle relocation, (d) acquisition of position and velocity.

3.5 Experimental Results

We explain that an observation color of the shuttle region is effective in the likelihood calculation of the badminton shuttle. A color reduction process is applied to the background image (as shown in Fig. 6(a_1)) and the observed color of the background image is plotted in the RGB space (Fig. 6(a_2) to obtain two representative colors (Fig. 6(a_3,) 6(a_4)). As for the observation color of the shuttle region observed with motion blur, a shuttle color (white) and a representative color of the background region (Fig. 6(a_4)) are blended. The observed color of the shuttle region is found on the straight line that connects the shuttle color (white) and the representative background color as shown in the RGB color space (Fig. 6(a_5), 6(a_6). In our proposed method, if a color blending is observed, we make a likelihood function in which the ellipsoid of the representative color and the white color is the observed color. Then we set the likelihood so that the color of the observed shuttle will be high. We get 30 shuttle regions of the outside and the inside shuttle region. Fig. 6(a_5) and 6(a_6) show the observation shuttle color in the RGB space. Each shuttle region is within the parameters of our model and various background colors are confirmed with effect by our model. As shown in Fig. 6, we conducted a proof experiment that compared the observation color of the shuttle region with the various background colors. The first experiment involved a green coat mat and background color (Fig. 6(a_1)–6(a_6). The second experiment involved a blue coat mat and background color (Fig. 6(b_1)–6(b_6). The last experiment involved the background color of the gymnasium (Fig. 6(c_1)–6(c_6). The distribution of the RGB values is the same as in the case described above. Therefore, the proposed method works effectively.

We evaluate the effectiveness of our proposed method using video sequences that were synchronously captured with two video cameras.

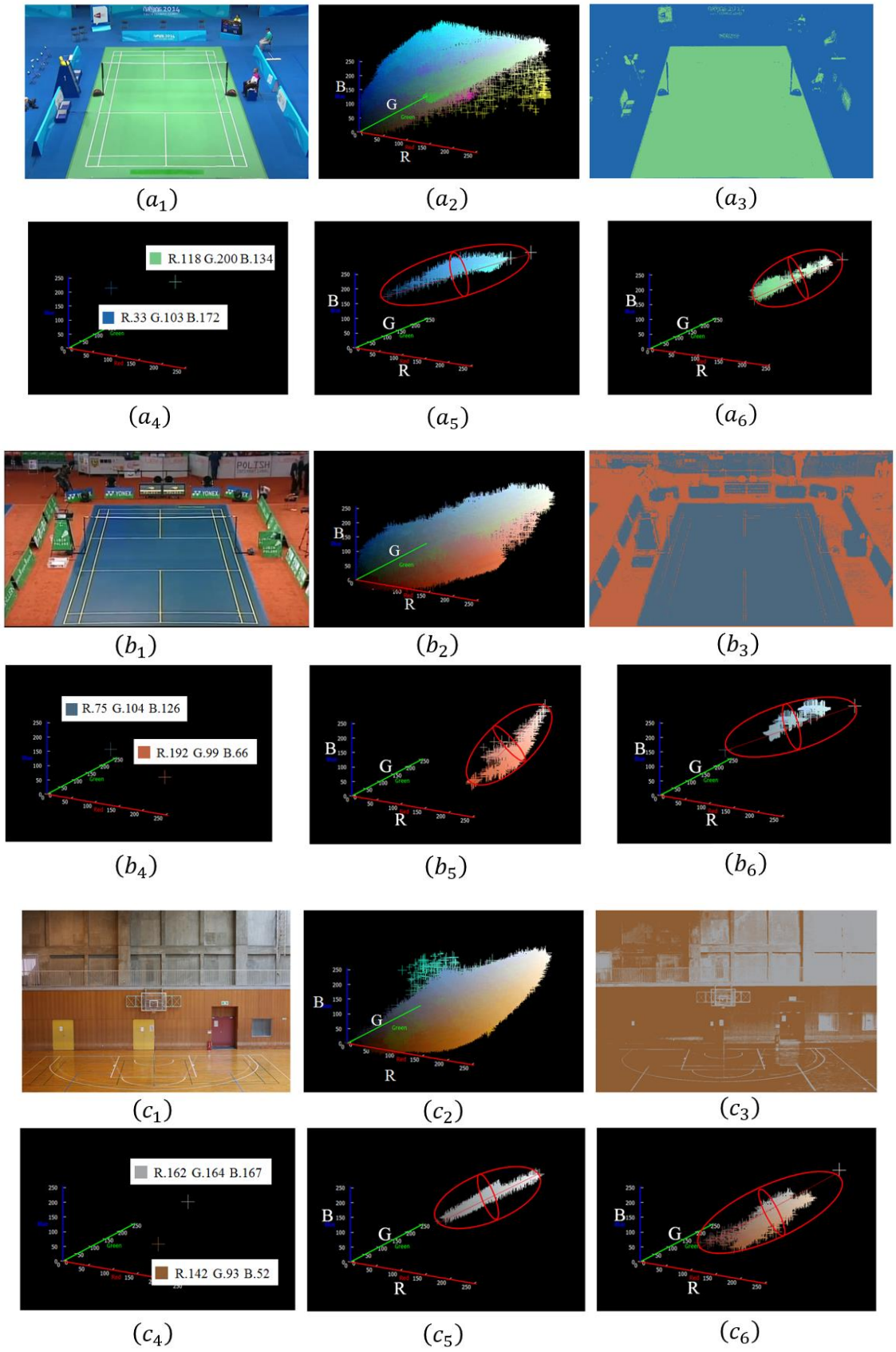

Fig. 6 The proof experiment that compared the observation color of the shuttle region with the various background colors. The proof experiment for the coat of mat green background color (a_1)–(a_6), the proof experiment for the coat of mat blue background color (b_1)–(b_6), the proof experiment for the background color of the gymnasium (c_1)–(c_6).

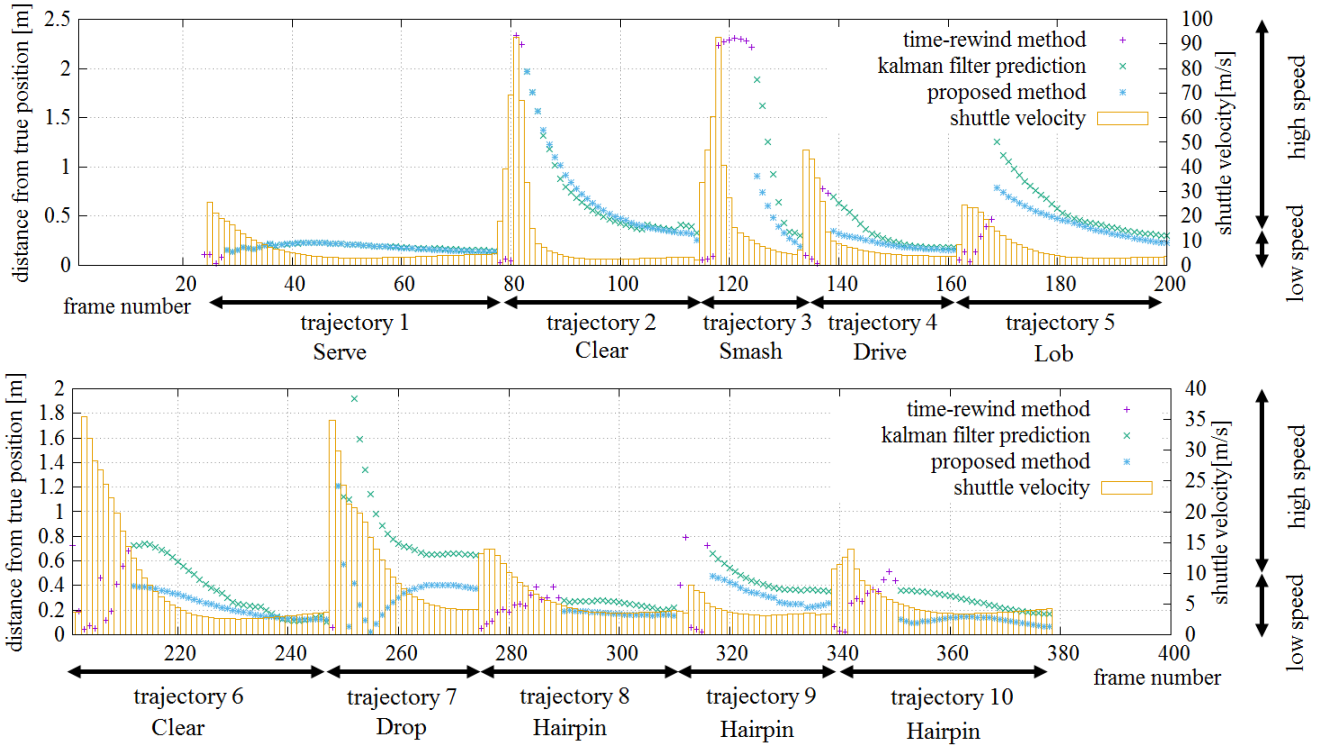

Fig. 7 Position estimation error across frames.

The multiple videos were captured using two digital single-lens reflex cameras (Canon EOS 5D Mark-II) with 1,920 × 1,080 pixels resolution, at 30 frames/sec. The shutter speed (exposure time) was set to 1/30 sec. Fig. 7 shows the estimation error calculated during ten racket strokes. This experimental result is a sequence that includes all types of shots. There are also a significant number of variations in velocity. The estimation error of the predicted position by the Karman filter is plotted as "×" and the estimated error by the proposed method is "✳". The above visual tracking process fails since, due to its quick movement, the detection of the shuttle and the Kalman filter construction is impossible in the early frames after the shuttle has been hit.

We mitigate this problem by rewinding the time-line from the initial observation frame (i.e., the first frame in which the Kalman filter works) to a former frame, only using the likelihood calculation (without the Kalman filter prediction step), as shown by "+." The error average is approximately 0.3 m. We estimated the object's 3D position based on the information obtained from two different viewpoints. As shown in Fig. 1, the 3D position (proposed method and ground truth) of the shuttle of all 10 orbitals was plotted from the result of Fig. 7.

When we capture badminton images, it is common to take an overhead view of the entire coat from a higher point, such as the second floor. Usually, the colors of the mat coats fall into the category shown in Fig. 6(a) or 6(c). Therefore, in many environments, the background region of the badminton sequence can be divided into two colors. The applicable condition is the environment divided into these two classes. Other than players and shuttles, dynamic objects are not reflected in the game images of badminton. When a dynamic object exists in the background, it is different from the size of the shuttle, therefore it can be excluded by image processing.

It is expected that a technology that provides 3D position information of the shuttle in badminton competition will be realized. Tactical analyses, in particular, are conducted by determining what kind of trajectory will be formed by the form of hitting. Specifically, the tactical analysis data can be divided into four types: [1] a pattern to take an ace, [2] a rally to take an ace, [3] a shot that is easy to error, and [4] a rally that is difficult for the other player[12]. The tactical analysis data of [1] to [4] are not required in detailing the information of the rally.

However, the type of rally will change if the estimation error exceeds 1 m in the environment of the facility in a

badminton competition. Therefore, it is considered to influence the tactical analysis. The 3D position estimation accuracy by this method has an average error of 0.3 m. We consider that this is within the range that can be fully utilized as tactical analysis data.

4. Trajectory Estimation Method for Badminton Shuttle Using Multiple Exposure Time Images

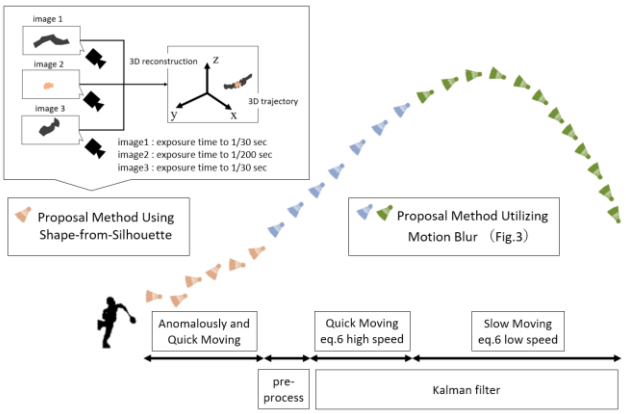

Fig. 8 Overall flow of the proposed method.

The verification experiments of our previously proposed method[13] were carried out in this paper and the validity was confirmed in Section 3. In addition, we proposed a new method by enhancing our previous research [13]. In the proposed method, it can be confirmed from the experimental result of the estimation error in Fig. 7. Because of the anomalous movement of the trajectory of the shuttle, as shown in Fig. 2, the error is large when the shuttle has just been returned. Therefore, focusing on the shuttle, which moves quickly and anomalously when it has just been returned, we describe the trajectory estimation method in Section 4.

As shown in Fig. 2 (a), the movement of the shuttle is anomalous for several frames just after striking and until the moving direction is stabilized. After that, we confirmed that the trajectory of the shuttle could be estimated by the method proposed in Section 3. In Section 4, we propose a trajectory estimation method at the beginning of the shot. The method proposed in Section 4 is applied at the beginning of the shot to estimate the position of the shuttle, along with the entire trajectory. After the movement direction is stabilized, the method of Section 3 is immediately applied (as shown in Fig. 8).

When estimating the 3D position of an object using images taken from multiple viewpoints, it is assumed that each image is taken synchronously. However, it frequently becomes difficult to capture synchronous images in a large space. By assuming a motion model, it is possible to approximately estimate the 3D position. However, it is difficult to fit a model when the object moves quickly and anomalously. Moreover, when capturing images of a shuttle, which moves quickly and anomalously in a large space, there is a challenge since the position and the orientation change anomalously while it simultaneously travels with rotation. By using captured images by multiple cameras with different exposure times, in this paper, we solve the problem of using asynchronous captured images and the problems that make trajectory estimations difficult due to diverse changes of the observation shape.

4.1 Trajectory Estimation Method Using Shape-from-Silhouette

By applying a 3D reconstruction method called shape-from-silhouette, in this section, we introduce our method for estimating the 3D position of a shuttle that does not follow a simple dynamic model. The shuttle was captured by two types of camera with different exposure times. Although it moves very quickly when its image is captured in a very short exposure time, it has little motion blur. In this case, the accuracy of the 3D position estimation is improved. On the one hand, the influence of the gap for capturing the timing becomes more serious (i.e., we need to completely synchronize all of the multiple cameras). On the other hand, if we capture a shuttle with a long exposure time, a large motion blur occurs since it is observed as a line in the image. In this case, although accurately estimating the position is difficult due to the uncertainty of the blur, the influence of the synchronizing error becomes smaller. Therefore, we propose a method that complementarily uses two types of cameras that capture different exposure times.

As shown in Fig. 9, the long exposure cameras (Cameras 1 and 3) are located at right angles to the Y- and X-axes, respectively. The short exposure camera (Camera 2) is located at right angles to the Y-axis. Each camera is calibrated in advance.

We extract the observation line from the clipped out region from the captured image shown in the upper space of Fig. 9(a), as a pre-process for the 3D reconstruction.

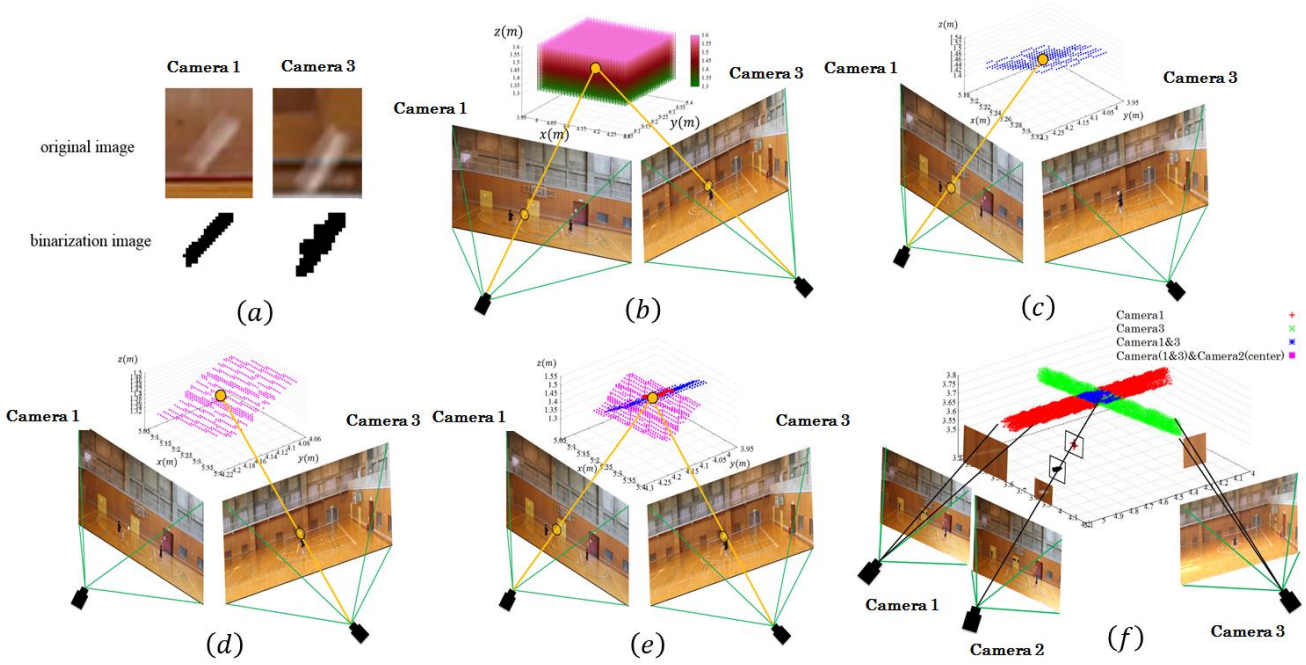

Fig.9 (a) Thinning process of shuttle region. (b) The 3D voxel space. (c) We project an element of the voxel onto Camera 1. When an observation line is not observed, we deleted the element from the voxel space. (d) We project an element of the voxel onto Camera 2. When an observation line was not observed, we deleted the element from the voxel space. (e) 3D trajectory estimation using shape-from-silhouette. The 3D shape of the observation line is estimated as a bunch of voxels. (f) The shuttle's 2D position, detected in the image captured by a short exposure time camera (Camera 2) is projected onto the 3D observation line.

In our developed system, the resolution of input image is 1,920 × 1,080 pixels and the observation size of a shuttle (motion blurred) region is about 30 × 30 pixels. Fig. 9(a) shows examples of the thinning process. We extract the silhouette image by executing background subtraction and binarization. Then, we extract the observation line by applying a thinning process to the binary image. This process is applied to multiple captured images. To estimate the 3D trajectory, we apply shape-from-silhouette to the extracted thinning image of the shuttle region (observation line). Here, all cameras are calibrated in advance. First, we set the 3D voxel space around the approximate 3D position of the shuttle, as shown in Fig. 9(b). In our system, according to the spatial-resolution of the captured image, the distance between each element of the voxel is set at 0.01 m. A voxel element is projected onto a captured image (e.g., Camera 1) by using camera parameters derived from the camera calibration results. Then, we examine whether an observation line exists at the projected position (pixel) or not and we delete the element if the observation line is not observed at the position, as shown in Fig. 9(c) and 9(d). To respond flexibly to projection error (i.e., camera calibration error), we set the thickness to the observation line. Specifically, we calculate the distance between the projected point and the observation line, and if the distance is less than a threshold, the point is regarded as existing on the observation line. In repeating a similar process with all of the other images, as shown in Fig. 9(e), we estimate the 3D shape of the observation line. The blue region of Fig. 9(f) shows a 3D observation line of the shuttle estimated by the observation of the long exposure image. Then the shuttle's 2D position, detected in the image captured by a short exposure time camera (Camera 2), is projected onto the 3D observation line. We can estimate the target shuttle's 3D position as intersection points.

4.2 Experimental Results

The multiple videos are captured using three digital single-lens reflex cameras (Canon EOS 5D Mark-II) with a 1,920 x 1,080 pixels resolution, at 30 frames/sec. The shutter speed (exposure time) is set to 1/30 sec (Fig. 9, Cameras 1 and 3) and 1/200 sec (Fig. 9, Camera 2), respectively. The badminton game is played in a gymnasium and if you set the shutter speed to be 1/200 seconds faster or more, it cannot obtain the shuttle region on the image due to the insufficient light source environment. Therefore, the short exposure time set in this study is defined as 1/200 sec. For the long exposure time, 1/30 second, which is the exposure time of general

photography, was selected. To apply the proposed method, it is necessary to shoot the short exposure time camera within the overlapping period of the plurality of the long exposure time cameras. Fig. 11 shows the proposed method using a video sequence. From the results in Fig. 11, we confirmed that the proposed method could be applied to video images. Specifically, we used badminton shuttle images taken at the actual gymnasium.

However, acquiring the shuttle's exact ground truth was difficult using only video. For that reason, we generated a 3D model of a badminton racket and a shuttle and conducted another experimental evaluation of our proposed method. A path similar to the shuttle trajectory of live-action video on blender was entered. We used the shuttle's 3D model to execute a CG animation on the path. In this way, we obtained the correct value of the shuttle and tested the estimation accuracy of the proposed method. The following are the characteristics of the shuttle's CG model: size (0.07 m). In Fig. 10, we animate the trajectory of one cycle of the shuttle. We set a virtual camera just like the one in the environment that captured the badminton shuttle. We generated shuttle motion blur in the blender, using the observed appearance in the past four frames. We precisely estimated the 3D position in both the video sequences and the CG animation. Fig. 12 shows the proposed method using a CG animation sequence and Fig. 13 compares the experimental results of the proposed and the previous methods[11]. Although the error average was approximately 0.04 m when applying our proposed method, it increased to approximately 0.07 m with the previous method. The error of our estimation accuracy is approximately 0.04 m, on average. As data for the purpose of improving tactics, it is a range that can be fully utilized. Therefore, we judged it to be effective.

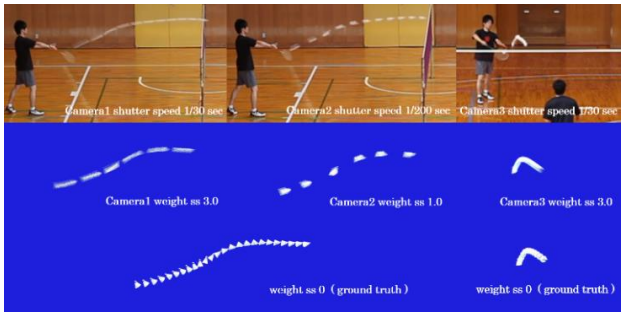

Fig. 10 CG simulation of badminton shuttle.

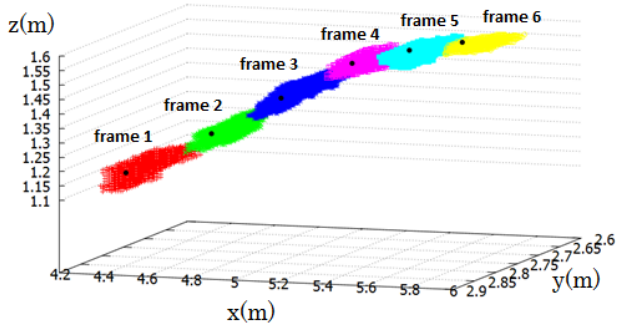

Fig. 11 Experimental results of video sequence.

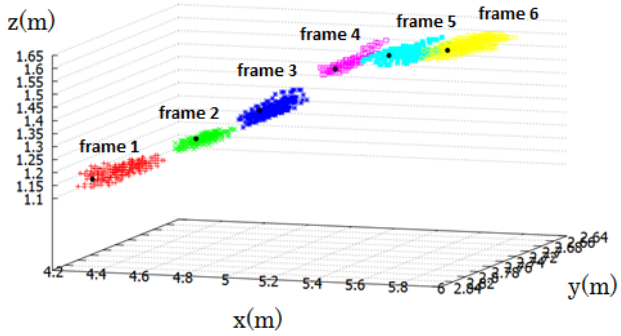

Fig. 12 Experimental results of CG animation.

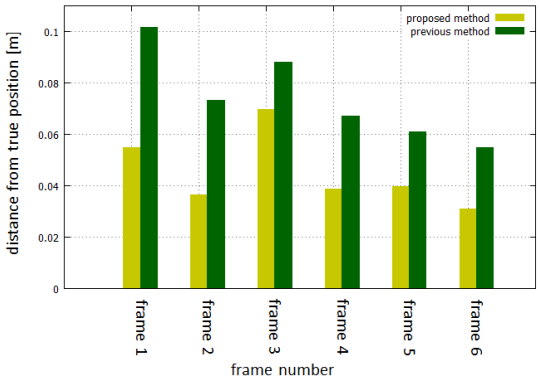

Fig. 13 Comparison of experimental results of proposed and previous techniques.

4.3 Potential for Sports Applications

In this research, we propose a method for moving the images of one rally. Therefore, when applying the proposed method to games, etc., the video must be manually divided by rally. However, since it is possible to estimate the 3D position of the shuttle in the proposed method, it is possible to detect the moment when the shuttle adheres to the ground. In addition, in badminton competition, there is a rule that the opposing player will be stationary when the other starts to serve. By using such competitive characteristics, we have the possibility of timing the detection of the rally start by

general image processing. However, to automate the proposed method against a series of competition images, such as with games, it is necessary to detect the moment when the shuttle adheres to the ground and the timing of the rally starts. By realizing this processing, it becomes possible to divide video by rally and apply the proposed method. In the proposed method, it is possible to estimate the 3D position of the moving object quickly and anomalously; the capturing condition makes it possible to estimate the 3D position even by using an asynchronous captured image.

In general, increasing the number of cameras increases the calculation cost. However, since our research is based on multi-view, the burden due to the increase in the number of cameras is relatively small. Specifically, when increasing the number of cameras, the merit of improving the estimation accuracy is larger than the increase in the calculation cost. Therefore, increasing the number of cameras that have the role of Camera 2 (short exposure time) will improve the accuracy. In addition, since there is a limit on the brightness of the actual gymnasium, there is a limit to shortening the exposure time of Camera 2. Therefore, except in special cases, improving the accuracy by shortening the exposure time is impossible and increasing the number of cameras is a practical method in sports applications.

5. Conclusion

This paper proposed a method of applying motion blur with shape-from-silhouette using multi-viewpoint imaging for the estimation of 3D trajectories for a badminton shuttle. To estimate the 3D trajectory of the observation line in the multiple-view image, we confirmed that the proposed method could estimate the 3D trajectory even when the shuttle moves very quickly and anomalously.

This work was supported by JSPS KAKENHI Grant Numbers 17K13180 and 25280056 and JST CREST Grant Number JPMJCR16E3, Japan.

References

1) F. Yan, W. Christmas, and J. Kittler: "Layered Data Association Using Graph-Theoretic Formulation with Application to Tennis Ball Tracking in Monocular Sequences," *IEEE Transactions on Pattern Analysis and Machine Intelligence,* 30, 10, pp. 1814–1830 (Oct. 2008)

2) H.-T. Chen, W.-J. Tsai, S.-Y. Lee, and J.-Y. Yu: "Ball Tracking and 3D Trajectory Approximation with Applications to Tactics Analysis from Single-camera Volleyball Sequences," *Multimedia Tools and Applications*, vol. 60, 3, pp. 641–667, (Oct. 2012)

3) J. Liu, P. Carr, R. Collins, and Y. Liu: "Tracking Sports Players with Context-Conditioned Motion Models," *Computer Vision and Pattern Recognition* (CVPR2013), pp. 1830–1837 (June. 2013)

4) F. Alam, H. Chowdhury, C. Theppadungporn, and A. Subic: "Measurements of Aerodynamic Properties of Badminton Shuttlecocks," *Procedia Engineering*, 2, 2, pp. 2487–2492 (June. 2010)

5) Y. Ding, S. McCloskey, and J. Yu: "Analysis of Motion Blur with a Flutter Shutter Camera for Non-linear Motion," In: *11th European Conference on Computer Vision* (ECCV2010), Lecture Notes in Computer Science, 6311, pp. 15–30 (2010)

6) H. Oku, N. Ogawa, K. Shiba, M Yoshida, and M. Ishikawa: "How to Track Spermatozoa Using High-Speed Visual Feedback," *30th Annual International Conference of the IEEE Engineering in Medicine and Biology Society Proceedings*, pp. 125–128 (Aug. 2008)

7) K. Okumura, H. Oku, and M. Ishikawa: "High-Speed Gaze Controller for Millisecond-order Pan/tilt Camera," *2011 IEEE International Conference on Robotics and Automation Conference Proceedings*, pp. 6186–6191 (May 2011)

8) Z. Wu, N.I. Hristov, T.L. Hedrick, T.H. Kunz, and M. Betke: "Tracking a Large Number of Objects from Multiple Views," *IEEE 12th International Conference on Computer Vision* (ICCV2009), pp. 1546–1553 (Sep 2009)

9) V. Reilly, H. Idrees, and M. Shah: "Detection and Tracking of Large Number of Targets in Wide Area Surveillance," *Computer Vision – ECCV 2010 Lecture Notes in Computer Science*, 6313, pp. 186–199 (2010)

10) L. Díaz-Más, R. Muñoz-Salinas, F.J. Madrid-Cuevas, and R. Medina-Carnicer: "Shape from Silhouette Using Dempster–Shafer Theory," *Pattern Recognition*, 43, 6, pp. 2119–2131 (June 2010)

11) K. Takanohashi, Y. Manabe, Y. Yasumuro, M. Imura, and K. Chihara: "Measurement of Ball Trajectory Using Motion Blur," *International Workshop on Advanced Image Technology*, P04–8, 2006

12) R. Savarirajan, and A.A. Govt: "An Analysis of Playing Pattern of Tamilnadu State Junior Badminton Players," *International Journal of Health, Physical Education and Computer Science in Sports*, 12, 1, pp. 24–27 (2013)

13) H. Shishido, I. Kitahara, Y. Kameda, and Y. Ohta: "A Trajectory Estimation Method for Badminton Shuttlecock Utilizing Motion Blur," *6th Pacific Rim Symposium on Image and Video Technology* (PSIVT'13), LNCS 8333, pp. 325–336 (2014)

Hidehiko Shishido

received his M.E. and Ph.D. degrees in Engineering from the University of Tsukuba, Japan, in 2013 and 2016, respectively. In 2015, he was visiting Ph.D. student at the Centre of Vision, Speech and Signal Processing, University of Surrey. In 2016, he served as a researcher at the Japan Institute of Sports Sciences. Since 2017, he has been an Assistant Professor at the University of Tsukuba. His research interests include computer vision and convolutional neural networks.

Yoshinari Kameda

received his B.E and M.E and Ph.D from Kyoto University in 1991, 1993, and 1999. He had a faculty position at Kyoto University in 1999-2003. He was a visiting scholar at MIT in 2001-2002. In 2003 he joined the University of Tsukuba and he is a professor at University of

Tsukuba. His research interests include the enhancement of human vision, augmented reality, mixed reality, video media processing, computer vision, and sensor fusion.

Yuichi Ohta

received his B.E. and M.E. degrees in Engineering from Kyoto University, Japan in 1972 and 1974, respectively. He received Ph.D. from Kyoto University in 1980. 1978-1981, he was Research Associate of Kyoto University. 1981-1987 Assistant Professor at the University of Tsukuba. 1987-1992 Associate Professor and 1992-2004 Professor at the University of Tsukuba. 2004-2009 Professor in the Graduate School of the University of Tsukuba. 2009-2012 he served as Provost of the Graduate School. 2013-2014, he was Vice President of the University of Tsukuba. 1982-1983, he was Visiting Scientist in Computer Science Department, Carnegie Mellon University. He is an IAPR Fellow, an IEICE Fellow, and an IPSJ Fellow.

Itaru Kitahara

received his B.E. and M.E. degrees in Science Engineering from University of Tsukuba, Japan in 1994 and 1996, respectively. In 1996, he joined Sharp Corporation. 2000-2003, he was a research associate of University of Tsukuba. He received his PhD in 2003. 2003-2005, he was a researcher at ATR. 2005-2008, he was an assistant Professor at the University of Tsukuba. Since 2008, he has been an associate professor at the University of Tsukuba. His research interests include computer vision, mixed reality, and intelligent image media.